

Demonstration of Scalability and Accuracy of Variational Quantum Linear Solver for Computational Fluid Dynamics

Ferdin Sagai Don Bosco*, Dhamotharan S†, Rut Lineswala‡, Abhishek Chopra§

BosonQ Psi (BQP) Corporation
New York, USA

* Senior Computational Scientist, Email: ferdindon@bosonqpsi.com

† Quantum Computing Developer

‡ Chief Technology Officer

§ CEO and Chief Scientific Officer, Email: abhishek.chopra@bosonqpsi.com

Abstract—The solution for non-linear, complex partial differential Equations (PDEs) is achieved through numerical approximations, which yield a linear system of equations. This approach is prevalent in Computational Fluid Dynamics (CFD), but it restricts the mesh size since the solution of the linear system becomes computationally intractable when the mesh resolution increases. The reliance on the ability of High-Performance Computers (HPC) to scale up and meet these requirements is myopic; such very high-fidelity simulations require a paradigm shift in computing. This paper presents an exploration of quantum methodologies aimed at achieving high accuracy in solving such a large system of equations.

Leveraging recent works in Quantum Linear Solver Algorithms (QLSA) and variational algorithms suitable for Quantum Simulation in HPC, we aspire to push the boundaries of CFD-relevant problems that can be solved on hybrid quantum-classical framework. To this end, we consider the 2D, transient, incompressible, viscous, non-linear coupled Burgers equation as a test problem and investigate the accuracy of our approach by comparing results with a classical linear system of equation solvers, such as the Generalized Minimal RESidual method (GMRES). Through rigorous testing, our findings demonstrate that our quantum methods yield results comparable in accuracy to traditional approaches. Additionally, we demonstrate the accuracy, scalability, and consistency of our quantum method. Lastly, we present an insightful estimation of the resources our quantum algorithm needs to solve systems with nearly 2 billion mesh points.

Index Terms—Quantum Computing, Variational Quantum Algorithm, Computational Fluid Dynamics, Partial Differential Equations

I. INTRODUCTION

Partial Differential Equations (PDE) are a powerful mathematical tool for describing the complex phenomena observed in all aspects of the universe. Its relevance in Science is evidenced through the Maxwell equations [1], Schrodinger equation [2], Engineering, evident from the Fourier heat transfer [3] and Navier-Stokes equations [4], and Finance, embodied by the Black-Scholes equation [5] is undeniable. Active research is constantly underway to discover new PDEs,

even with the aid of data-driven techniques, such as Physics-Informed Neural Networks (PINNs) [6].

However, describing a physical phenomenon is only the first challenge; solving it is even more daunting. This is often insurmountable, especially when the PDE features non-linearity (Burgers equation [7]), incomplete closure (Navier-Stokes equations), or is very complex, such as the integro-differential nature of the Boltzmann equation [8].

Non-linear PDEs are specifically prominent in transport mechanics, with applications including plasma fields [9], nanofluid flow [10], and shallow water waves [11]. Fluid dynamics and the associated field of Computational Fluid Dynamics (CFD) possess a rich ensemble of such PDEs, which capture complex physical phenomena, such as convection-diffusion, heat transfer, shock wave formation and propagation, etc. However, an analytical solution is only feasible for a grossly simplified version of the original phenomena, which is of little real-world importance.

This has engendered an appetite for numerical recipes that simplify the PDE into a system of algebraic equations. In CFD, for instance, the process of solving the system of PDEs is depicted in Fig. 1. It begins by identifying a set of PDEs that describe the observed flow behaviour as the governing equation. Initial conditions and boundary conditions are then specified as dictated by the physics of flow. Since these equations follow the laws of continuum mechanics, the conversion of the governing PDEs to the algebraic system of equations is popularly achieved through grid-based methods, such as the Finite Difference Method (FDM) [12], Finite Volume Methods (FVM) [13] or Finite Element Method (FEM) [14]. The chosen method determines the manner in which the flow domain is viewed; in FDM, it is distributed collocation points, while in FVM it is interconnected volumes, whereas FEM views the domain as interlinked elements. In transient flow, the strategy employed for time integration often addresses the non-linearity. Explicit method solves each discretized domain one at a time, while the implicit method involves solving the entire

system of equations simultaneously, where both the linear and nonlinear terms are treated implicitly. On the other hand, a semi-implicit method combines aspects of both explicit and implicit methods, typically treating the linear terms implicitly and the nonlinear terms explicitly [15]. Implicit and Semi-implicit methods are generally utilized as it solves the entire domain simultaneously. With these methods, irrespective of the means, the end result is a linear system of equations, which can be expressed as $\mathbf{Ax} = b$ (Fig. 1).

It is crucial to note that nearly all PDE systems can be simplified to the above linear system. Consequently, there have been multi-disciplinary efforts to solve the system, which has led to a plethora of methods, direct (Gaussian Elimination, Thomas Algorithm), iterative (Gauss-Seidel, Gauss Jacobi), and Krylov subspace (Conjugate Gradient, Generalized Minimal Residual) methods [16], being developed and utilized over the past several decades. Recent times have also witnessed the rise of code libraries, such as NumPy [17], Intel's MKL [18], etc., with significant efforts going into accelerating the solution to $\mathbf{Ax} = b$. These methods and implementations have also efficiently handled very large systems.

However, in certain CFD studies such as a Direct Numerical Solution (DNS) for turbulence [19], the mesh sizes desired are very small (on the order sub-Kolmogorov scale [20]). This leads to massive $\mathbf{Ax} = b$ systems that are computationally intractable even with the formidable throughput offered by the modern Exascale supercomputers.

While the previous generations had the option to wait till computational power increased to meet their need, we do not have that luxury. Modern technology is quickly approaching the limit of Moore's law, physically [21] and economically [22].

In general, the ultimate aim of computational methods is to provide real-time predictions of the complex physical phenomena being modelled. Such a capability elevates such computational tools from merely a design tool kit to a step towards true virtualization. However, such a vision requires immense computational power, which must be a result of a paradigm shift in computing.

Significant faith is placed in Quantum Computers (QC), which are, theoretically, capable of solving large systems with enormous acceleration [23]. Numerous algorithms have been devised for the solution of the Navier-Stokes system of equations, many of which have been discussed in detailed reviews by Gaitan [24], [25]. A few of these approaches are focussed on quantum acceleration of traditional Navier-Stokes solution strategies, such as Finite Difference Methods (FDM), Finite Volume Methods (FVM) [26], and Finite Element Methods (FEM) [27]. A larger volume of research has been dedicated to quantum approaches to the Lattice Boltzmann Methods (LBM) [28]–[30].

Any claim of quantum supremacy can only be established once quantum computers of meaningful capacity have been constructed [31]. Meanwhile, our understanding garnered from existing quantum machines can be gainfully utilized to create hybrid algorithms [32] capable of running on such hardware.

The advent of quantum simulators has given an impetus to the quantum algorithm and code development efforts. It is now feasible to test out the efficacy of a computational algorithm on large emulations of quantum hardware [33], [34], essentially preparing for a time when, inevitably, quantum computers become a reality. Such attempts are historically poetic and reminiscent of Ada Lovelace's efforts to develop code for digital silicon-based computers that didn't exist yet [35], [36].

There have been attempts in the quantum field to develop algorithms for the solution of a linear system ($\mathbf{Ax} = b$) on quantum hardware. One of the original approaches was the Harrow–Hassidim–Lloyd (HHL) algorithm [37] which achieved an exponential acceleration over contemporary classical algorithms. Further improvement on the algorithm's precision was obtained by utilizing Quantum Singular Value Transformations (QSVT) [38], such as the method proposed by Childs, et. al [39]. However, it is critical to recognize that these speed-ups do not consider the state preparation and state readout requirements, which are themselves, quite challenging. Moreover, these algorithms are meant to be used for fault-tolerant hardware, which is still a few years away. Even those designed for hybrid architectures [40] exhibit discouraging performance on quantum simulators in terms of number of qubits (and circuit depth) [41].

Another promising approach, specifically in the Noisy Intermediate-Scale Quantum (NISQ) era, is the Variational Quantum Linear Solver (VQLS) [42], which has found remarkable success and has also been utilized to solve heat conduction equation [43] and Poisson equation [44], [45]. However, the VQLS algorithm, being a variational algorithm, loses coherence during the computation due to the measurement of the cost function. This loss of coherence limits the potential quantum advantages that can be harnessed.

This drawback is largely mitigated by the Coherent Variational Quantum Linear Solver (CVQLS), which combines strengths of Variational Quantum Algorithm (VQA) and classical linear algebra. The CVQLS distinguishes itself from the VQLS in three distinct aspects. Firstly, the VQLS utilizes a more general framework for solving optimization problems using quantum computers, while, CVQLS leverages quantum coherence to enhance the accuracy and efficiency of the solution. Secondly, CVQLS encodes the linear system into a quantum state using a coherent process, while VQLS utilizes different embedding techniques. Lastly, the cost function in CVQLS is typically designed for linear systems, while VQLS can use more general cost functions.

Hybrid quantum-classical algorithms are aptly suited to the present NISQ-era and similar methods have been used to solve equations relevant to CFD, such as the Poisson equation [46], [47].

This research work utilizes such a hybrid quantum-classical method, in which CVQLS is used as a quantum linear solver algorithm (QLSA), which works well for current quantum computers/simulators. The algorithm, Hybrid Quantum-Classical Finite Methods (HQCFM), can solve $\mathbf{Ax} = b$ while maintaining high accuracy, consistency and scalability. The

HQCFM algorithm give more coherent and precise probability distribution for the solution vector, thereby potentially offering greater quantum speedups.

These claims are put to the test by solving the 2D, transient, incompressible, viscous, non-linear, coupled Burgers equation described in Section II. Section III briefly describes the methodology utilised in this research. The accuracy, scalability, and consistency of HQCFM is established in Section IV. Section V utilizes the knowledge gained in the simulation of the Burgers equation to develop predictive models that provide insight into the cost associated with extending the HQCFM to complex, real-world problems. Fig. 1 clarifies this paper's focus and the exact field where HQCFM will make an impact.

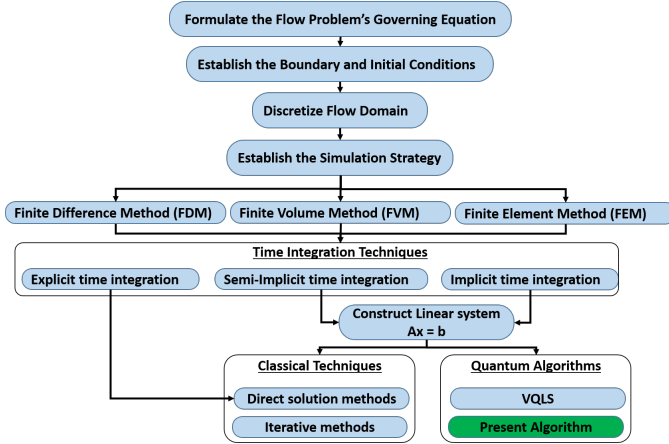


Fig. 1: Focus of the present research article.

II. PROBLEM DEFINITION

A. Significance of the problem

One of the most celebrated nonlinear partial differential equations in the field of fluid mechanics is the Burgers equation [7]. It is a model equation that is capable of capturing the interaction between advection and diffusion. It arises in gas dynamics, traffic flow, chromatography and flood waves in rivers.

Due to its similarity with the Navier-Stokes equation, it is considered an important model for testing numerical algorithms for the Navier-Stokes equation. The numerical solution of this equation is an indispensable tool for studying incompressible fluid flow problems.

B. Formulation

The Burgers equation is a highly regarded model equation in the field of CFD. It has been shown to model turbulence [48] and propagation shockwave in viscous fluids [49], [50].

The 2D governing equations are,

$$\frac{\partial u}{\partial t} + u \frac{\partial u}{\partial x} + v \frac{\partial u}{\partial y} = \frac{1}{Re} \left[\frac{\partial^2 u}{\partial x^2} + \frac{\partial^2 u}{\partial y^2} \right] \quad (1)$$

$$\frac{\partial v}{\partial t} + u \frac{\partial v}{\partial x} + v \frac{\partial v}{\partial y} = \frac{1}{Re} \left[\frac{\partial^2 v}{\partial x^2} + \frac{\partial^2 v}{\partial y^2} \right] \quad (2)$$

For this article, the initial conditions are taken as,

$$\begin{aligned} u(x, y, 0) &= \sin(\pi x) + \cos(\pi y) \\ v(x, y, 0) &= x + y \end{aligned} \quad (3)$$

and the boundary conditions as,

$$\begin{aligned} u(0, y, t) &= \cos(\pi y) & u(L_x, y, t) &= 1 + \cos(\pi y) \\ v(0, y, t) &= y & v(L_x, y, t) &= 0.5 + y \\ u(x, 0, t) &= 1 + \sin(\pi x) & u(x, L_y, t) &= \sin(\pi x) \\ v(x, 0, t) &= x & v(x, L_y, t) &= 0.5 + x \end{aligned} \quad (4)$$

The square domain with $L_x = L_y = 0.5$ is chosen for the study. The numerical computations are performed on a uniform grid whose cell size depends on the chosen grid resolution. The Reynolds number, Re , is chosen to be 50. The solution time is chosen to be 0.625, and time steps are chosen appropriately. The Cartesian discretization and boundary conditions schematic is illustrated in Fig. 2.

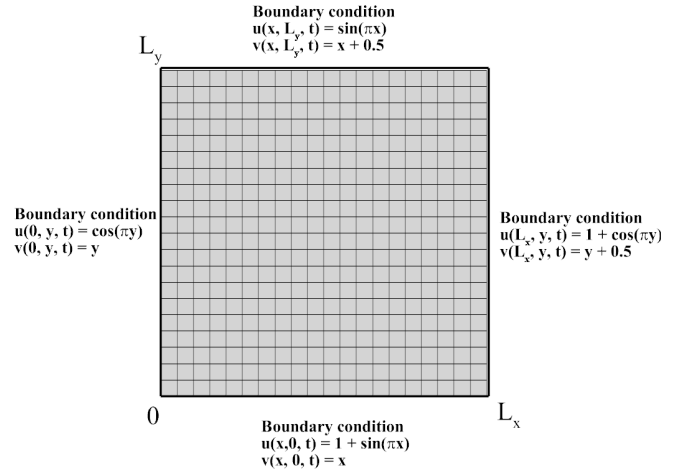


Fig. 2: Schematic of the computational domain.

The spatial discretization and time integration scheme used by Srivastava and Tamsir [48] are chosen here. Studies [51], [52] demonstrate through stability analysis and numerical experiments that semi-implicit schemes exhibit superior stability properties compared to explicit schemes. While implicit methods solve the entire system simultaneously, semi-implicit methods strike a balance between explicit and implicit treatments of different terms within the equations. Semi-implicit methods are often favored for improved stability, especially when dealing with complex systems involving linear and nonlinear components. Thus, the semi-implicit scheme is used for this study.

The discretization results in the creation of two linear systems corresponding to u and v velocities, which must be solved at each time step. Thus,

$$\begin{aligned} [A]u^{t+\Delta t} &= u^t \\ [A]v^{t+\Delta t} &= v^t \end{aligned} \quad (5)$$

The above linear system is solved once for each velocity component. Thus, in a single time step, 2 linear system solutions are obtained.

The entire process is outlined in Fig. 3.

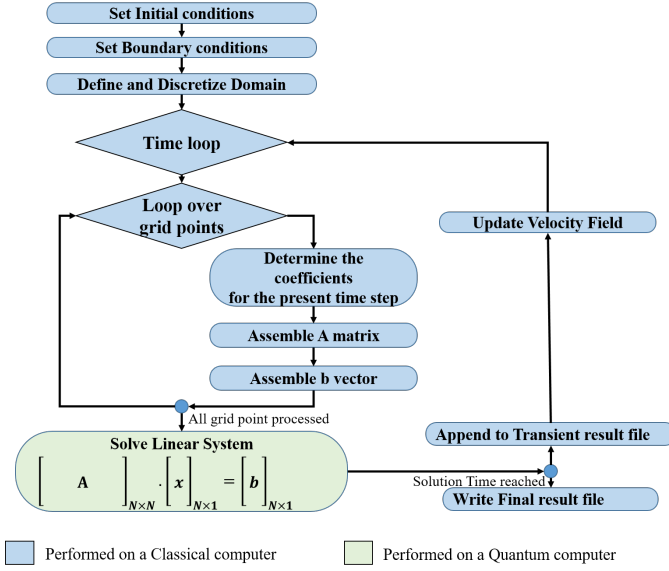


Fig. 3: Flowchart for the present HQCFM algorithm.

C. Setup

The size of the square matrix $[A]$ is referred to as system size. It is related to the number of grid points in the X and Y direction as, $n_x = n_y = \sqrt{N}$, where N is the size of the $[A]$ matrix. Thus, a grid of 8×8 corresponds to a system size of 64. An artifact of HQCFM and other quantum algorithms is the need for the system sizes to be powers of 2. If this is not the case, then padding is utilized to ensure the system meets the criteria. This padding is a numerical fix and doesn't affect or alter the solution in any way. The size of matrices studied in this research is presented in Tab. I.

III. METHODOLOGY

A. Iterative Classical PDE Solver

The classical solver is used to provide a basis for comparison for the HQCFM. The discretization process and the assembly of the $Ax = b$ system remain identical for both methods. The classical and HQCFM perform all the blue boxes in Fig. 3. However, instead of solving the linear system through HQCFM (green box in Fig. 3), the classical solver utilizes an established classical method, namely, the Generalized Minimal RESidual method (GMRES), further details of which can be found in a recent review by Zou [53].

B. Iterative Quantum PDE Solver

This work leverages a Quantum Linear System Algorithm (QLSA) well-suited for the NISQ era. We modified an existing QLSA to solve the system of linear equations arising at each time step for semi-implicit discretization of the 2D, transient, incompressible, viscous, non-linear, coupled Burgers

equation. As depicted in Fig. 1, the solution of any partial differential equation (PDE) involves solving a system of the form $Ax = b$. We exploit the fact that the A matrix in this system can be decomposed into a linear combination of unitary matrices. This decomposition allows us to embed these matrices efficiently onto a quantum circuit within a Variational Quantum Algorithm (VQA) framework to reach the target state $|\psi\rangle$. The process of our HQCFM can be summarized as follows,

- We decompose our A matrix using spectral theorem as in "Matrix Analysis" by Roger A. Horn and Charles R. Johnson. [54]
- Calculating the Euclidean norm of difference between Quantum $|b\rangle$ and Classical b , using this cost for the optimization process.
- After finding the best θ (variational) parameters for the circuit, we prepare our x vector.
- We have utilized IBM Qiskit AerSimulator (GPU-enabled).

IV. RESULTS AND DISCUSSION

In this section, the accuracy of the HQCFM is established by comparing it with classical solver results. The scalability is then tested by using finer mesh sizes. Finally, comments are made regarding the consistency of the HQCFM by studying the difference between its solution and classical solution at every time step.

A. Accuracy

The velocity contours for the transient solution of the 2D, transient, incompressible, viscous, non-linear, coupled Burgers equation are depicted in Fig. 4. These results were obtained using the HQCFM introduced in this paper to solve the linear system at every time step. Such a demonstration of using a quantum linear equation solver coupled with a transient problem is unprecedented. Moreover, the results obtained also match the expected flow field for the Burgers' equation with the initial and boundary conditions specified in the problem statement (refer section II-B) [48].

In order to better appreciate the accuracy of HQCFM, we ran identical cases using the classical solver introduced in Section III-A. The resulting contours from the HQCFM and classical solver were subtracted from one another to produce a difference plot as shown in Fig. 5. Here, Fig.5a plots the difference in the computation of the X velocity component between classical and the HQCFM, while Fig. 5b depicts the difference Y velocity component.

It can be observed that the maximum disagreement between the two occurs in the top right region of the domain. Although a discrepancy is noted, the difference is very small, on the order of e^{-5} . The tables present the physics-based validation of the results, II and III. In these tables, the values of the u and v velocity at specific points are compared with those reported in the literature. Minor disagreements are observed, but these can be adequately explained. The discrepancy with respect to Srivastava [48] arises because of different grid sizes.

TABLE I: Size of the matrix systems used in this study.

Actual System Size ($N \times N$)	Grid Resolution ($n_x \times n_y$)	Padding	System Size after Padding ($N \times N$)
16 x 16	4 x 4	False	16 x 16
25 x 25	5 x 5	True	32 x 32
64 x 64	8 x 8	False	64 x 64
121 x 121	11 x 11	True	128 x 128
256 x 256	16 x 16	False	256 x 256
484 x 484	22 x 22	True	512 x 512
1024 x 1024	32 x 32	False	1024 x 1024
2025 x 2025	45 x 45	True	2048 x 2048

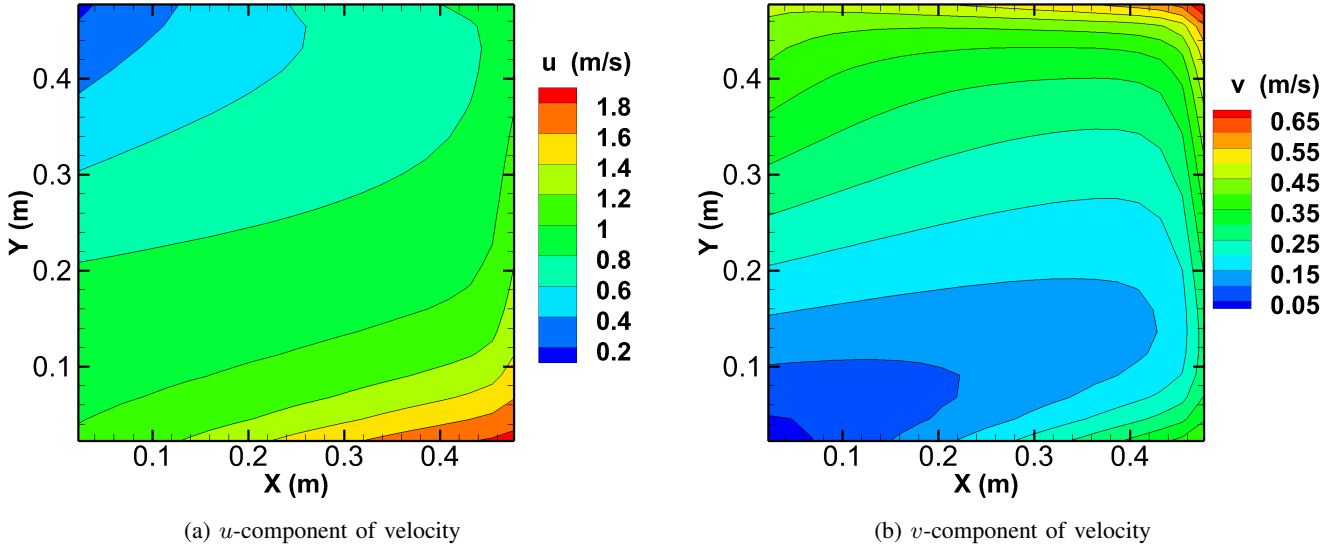


Fig. 4: Contour plots of velocity components and magnitude for a 2D, transient, incompressible, viscous, non-linear, coupled Burgers equation with a 512×512 size system.

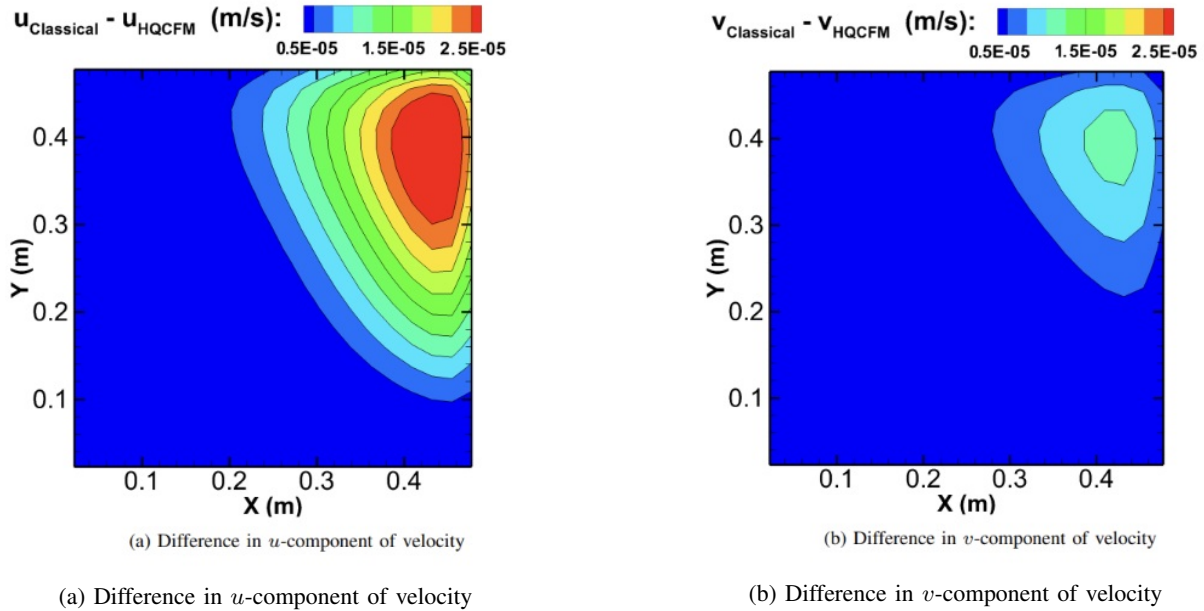


Fig. 5: Contour plots of velocity components and magnitude between classical and quantum solver for a 2D, transient, incompressible, viscous, non-linear, coupled Burgers equation with a 512×512 size system.

The results presented are for a 22×22 grid, whereas those in the reference are for a 20×20 grid. On the other hand, the present approach is semi-implicit, whereas that reported in Bahadir [55] is fully implicit. The mismatch is consequently, a result of the difference in the treatment of the non-linearity, hence these differences can be attributed to the numerics.

B. Scalability

Although the accuracy of the quantum linear system solver with regards to the classical solver has been established for a 512×512 sized system, this is not the top limit. In fact, a number of other simulations with variations in the system size have also been performed to gauge the scalability properties of the HQCFM. The accuracy of these simulations is presented in terms of the L2 norm between the HQCFM and classical results in Fig. 6a. It is observed that the L2 norm is in the range of $1e^{-5}$ to $1e^{-11}$, nearing machine zero, even for systems as large as 2048. This provides enormous confidence in the ability of the developed quantum solver to scale up to larger problems.

Accuracy alone is not the only factor affecting scalability. Quantum algorithms require a number of qubits to be held in a superposition state, which is a physically arduous process. The number of qubits increases with the system size. In the present research, the number of qubits used by the algorithm for each of the systems is measured and plotted in Fig. 6b. A more robust breakdown of the number of qubits and quantum gates is provided in Tab. IV.

C. Consistency

It is worth reiterating that this article demonstrates the developed capability of HQCFM, achieving not only high accuracy and scalability but also exhibiting remarkable consistency in these features. Notably, the quantum solver is integrated into the time loop, requiring evaluation at every time step for the Burgers' equation. This equation's non-linear nature necessitates re-evaluation of the coefficient matrix, \mathbf{A} , based on the previous step's results at each iteration. This emphasizes the critical need for the HQCFM to maintain consistent accuracy throughout the simulation, as any errors can propagate and significantly alter the trajectory toward the steady-state solution. However, as Fig. 7 illustrates, the solutions obtained using the HQCFM and the classical solver exhibit near-identical convergence behavior towards the steady state. This consistency highlights the effectiveness of the HQCFM in maintaining accuracy even under the iterative nature of the time-stepping algorithm.

V. RESOURCE ESTIMATION

The resources utilized by the HQCFM are listed in Tab. IV for the simulations performed in this research. These are crucial for trying to predict resources required for larger simulation systems.

Consider a complex problem like internal flow in turbomachinery, which is characterized by non-linearity and turbulence. Such a flow can only be resolved by high mesh

sizes and significant computational power. For a mesh of size 2^{30} , or approximately 1.69 billion cells, a traditional high-performance computer (HPC) system would require about 19.2 million cores [56].

When the HQCFM presented in this research is run on an ideal quantum computer, this same problem could be tackled using only 30 qubits. However, it is also paramount that we have an estimate of the Quantum resources the HQCFM would utilize to run such a simulation. Such a resource estimation exercise is performed here using an arithmetic progression model based on the data gathered in Tab. IV.

An arithmetic progression model can estimate the number of single qubit gates, as depicted in Eq. 6.

$$a_n = a_1 + (n - 1) d \quad (6)$$

Here, a_n is the number of single qubit gates required for simulating the target system size, a_1 is the starting point, which is taken to be the 16×16 system. Thus, by consulting the table $a_1 = 76$. Additionally, n is the number of qubits, and d is the difference between two consecutive systems, which is obtained by taking the difference between consecutive systems' single qubit gate requirement. From consulting the tab. IV, $d = 19$.

Thus, for a $n = 30$, the number of single qubits gates utilized by HQCFM would be $76 + (29) \times 19 = 627$

The number of multi-qubit gates can also be estimated by an arithmetic progression model, as depicted in Eq. 7.

$$d_n = d_1 + (n - 1) d$$

$$a_n = a_1 + \sum_{k=1}^{n-1} d_k \quad (7)$$

After rewriting

$$a_n = a_1 + \frac{(n - 1)(d_1 + d_n)}{2} \quad (8)$$

From consulting Tab. IV, the value of $a_1 = 42$, $d_1 = 24$, and the common difference of differences, $d = 6$. Here, d_n is computed first using Eq. 7, as $d_n = 24 + (29) \times 6 = 198$. Thus, for a $n = 30$, the number of multi-qubits gates utilized by HQCFM would be obtained from Eq. 8 as, $a_n = 42 + (29) * (24 + 198)/2 = 3261$.

Thus, it would take 627 single-qubit gates and 3261 multi-qubit gates, totalling 3882 gates, for the HQCFM to perform the internal, turbulent flow inside a turbomachinery device using a grid with 1.69 billion cells. Thus, the HQCFM offers a reduction in hardware requirements compared to traditional HPC while also enabling highly complex simulations.

VI. CONCLUSION

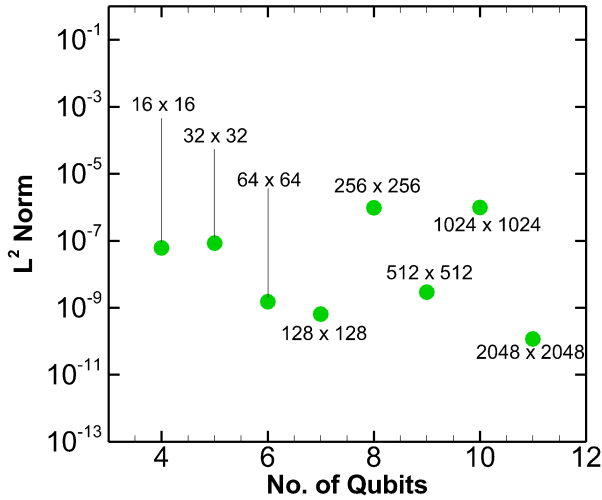
The rising demand for true virtualization, either through digital twins or real-time solutions, combined with the surging size and complexity of the associated Partial Differential Equations (PDEs) has challenged and outpaced the existing High Performance Computers. With the onset of the Moore

TABLE II: Comparison of computed values of u from HQCFM and Classical Solver against literature for $Re = 50$ at $t = 0.625$.

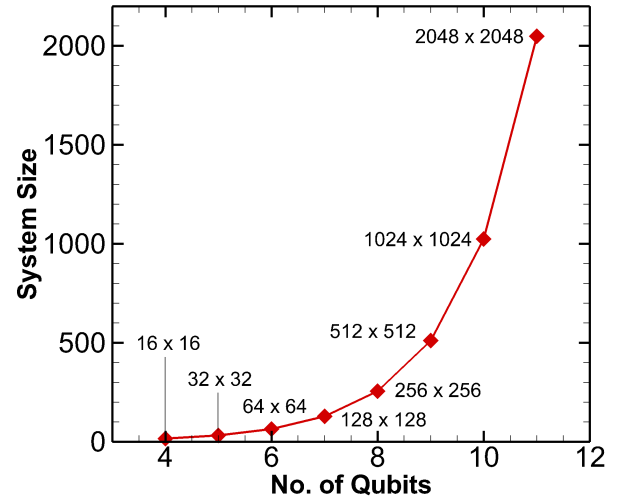
X(m)	Y(m)	HQCFM	Classical	Srivastava [48]	Bahadir [55]
0.1	0.1	0.962570961	0.962571185	0.97146	0.96688
0.3	0.1	1.096567222	1.096580234	1.1528	1.14827
0.2	0.2	0.861248176	0.861256984	0.86307	0.85911
0.4	0.2	0.939141661	0.939266899	0.97981	0.97637
0.1	0.3	0.664038717	0.664042106	0.66316	0.66019
0.3	0.3	0.764007634	0.76410028	0.7723	0.76932
0.2	0.4	0.581100144	0.581146485	0.5818	0.57966
0.4	0.4	0.748058121	0.748329615	0.75855	0.75678

TABLE III: Comparison of computed values of v from HQCFM and Classical Solver against literature for $Re = 50$ at $t = 0.625$.

X(m)	Y(m)	HQCFM	Classical	Srivastava [48]	Bahadir [55]
0.1	0.1	0.093884394	0.093884452	0.09869	0.09824
0.3	0.1	0.118062887	0.118066365	0.14158	0.14112
0.2	0.2	0.16395324	0.163956008	0.16754	0.16681
0.4	0.2	0.157233779	0.15727113	0.17109	0.17065
0.1	0.3	0.264646384	0.264647809	0.26378	0.26261
0.3	0.3	0.224208984	0.224244041	0.22654	0.22576
0.2	0.4	0.314125289	0.314146998	0.32851	0.32745
0.4	0.4	0.305482011	0.305587781	0.32499	0.32441



(a) Variation of accuracy for various systems sizes w.r.t. number of qubits



(b) Scalability of system size with number of qubits

Fig. 6: Demonstration of scalability and accuracy of HQCFM for a 2D, transient, incompressible, viscous, non-linear, coupled Burgers equation.

limit, the hope that silicon-based computers can address these need is fading. Next-generation technologies are needed to satisfy current demand and sustain the course of scientific enquiry into the future. Quantum computing, is one of the few options that shows tremendous promise.

In this article, the Hybrid Quantum-Classical Finite Method (HQCFM) is developed based on an existing Quantum Linear Solver Algorithm (QLSA). The focus of the HQCFM was to solve the $\mathbf{A}x = b$ linear system, which is utilized in the present research to solve 2D, transient, incompressible, viscous, non-linear, coupled Burgers equation. Such a demonstration of using a quantum linear equation solver coupled with a transient

problem is unprecedented. The performance of HQCFM is measured using 3 metrics, viz., Accuracy, Scalability, and Consistency,

Present results indicate a very high accuracy when compared to classical solvers. The results are also verified with those reported in the literature. Various system sizes are used to judge the scalability of HQCFM. The results indicate a good scale-up behavior. Quantitative information regarding the scale-up is also provided in terms of qubits and quantum gates utilized. The HQCFM also distinguishes itself by running inside a time loop in a transient problem, without propagating any error to the next time step. Obtaining such a high accuracy consistently

TABLE IV: Resources utilized by the HQCFM quantum circuit for different system sizes. Value in the brackets is the no. of Cx gates out of the total multi-qubit gates.

Size of the System	No. of Qubits	No. of Single Qubit Gates	No. of Multi-Qubit Gates (No. of Cx gates)	Total Gates
16	4	76	42 (Cx = 36)	118
32	5	95	66 (Cx = 60)	161
64	6	114	96 (Cx = 90)	210
128	7	133	132 (Cx = 126)	265
256	8	152	174 (Cx = 168)	326
512	9	171	222 (Cx = 216)	393
1024	10	190	276 (Cx = 270)	466
2048	11	209	336 (Cx = 330)	545

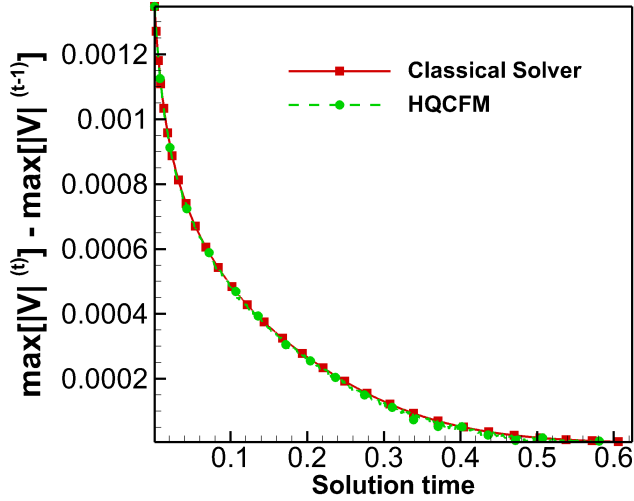


Fig. 7: Variation of maximum magnitude of velocity in consecutive time steps with solution time for quantum and classical solvers.

in a system of linked linear systems is a major breakthrough in the field of quantum computing.

Apart from these scientific findings, this paper also explores the economical aspect of quantum computing. A robust resource estimation, based on information gathered in this research, is used to predict the resources needed by HQCFM to perform complex real-world simulations. These predictions indicate that a 30-qubit quantum computer will be able to outperform an Exascale computer.

ACKNOWLEDGMENT

The authors would like to thank Mr. Abhishek Singh (HPC Engineer at BosonQ Psi) and Mr. Aman Mittal (HPC Engineer at BosonQ Psi) for their support with computational resources; Mr. Akshith Chowdary (Quantum Software Developer at BosonQ Psi) and Mr Aakif Akthar (Quantum Algorithm Developer at BosonQ Psi) for their keen insights and oversight during the writing process; Dr. Kandula Eswara Sai (Senior Optimization Scientist at BosonQ Psi) for guidance and support.

REFERENCES

- [1] Allen Taflove and Morris E Brodwin. Numerical solution of steady-state electromagnetic scattering problems using the time-dependent maxwell's equations. *IEEE transactions on microwave theory and techniques*, 23(8):623–630, 1975.
- [2] Gadí Fibich. *The nonlinear Schrödinger equation*, volume 192. Springer, 2015.
- [3] Thiruppudaimarudhur N Narasimhan. Fourier's heat conduction equation: History, influence, and connections. *Reviews of Geophysics*, 37(1):151–172, 1999.
- [4] Roger Temam. *Navier-Stokes equations: theory and numerical analysis*, volume 343. American Mathematical Soc., 2001.
- [5] Guy Barles and Halil Mete Soner. Option pricing with transaction costs and a nonlinear black-scholes equation. *Finance and Stochastics*, 2:369–397, 1998.
- [6] Hao Xu and Dongxiao Zhang. Robust discovery of partial differential equations in complex situations. *Physical Review Research*, 3(3):033270, 2021.
- [7] Mayur P Bonkile, Ashish Awasthi, C Lakshmi, Vijitha Mukundan, and VS Aswin. A systematic literature review of burgers' equation with recent advances. *Pramana*, 90:1–21, 2018.
- [8] Carlo Cercignani and Carlo Cercignani. *The boltzmann equation*. Springer, 1988.
- [9] Aly R Seadawy. Solitary wave solutions of two-dimensional nonlinear kadomtsev–petviashvili dynamic equation in dust-acoustic plasmas. *Pramana*, 89:1–11, 2017.
- [10] M Sheikholeslami and AJCMIAM Zeeshan. Analysis of flow and heat transfer in water based nanofluid due to magnetic field in a porous enclosure with constant heat flux using cvfem. *Computer Methods in Applied Mechanics and Engineering*, 320:68–81, 2017.
- [11] Aly R Seadawy. Travelling-wave solutions of a weakly nonlinear two-dimensional higher-order kadomtsev-petviashvili dynamical equation for dispersive shallow-water waves. *The European Physical Journal Plus*, 132:1–13, 2017.
- [12] M Necati Özişik, Helcio RB Orlande, Marcelo J Colaço, and Renato M Cotta. *Finite difference methods in heat transfer*. CRC press, 2017.
- [13] Fadl Moukalled, Luca Mangani, Marwan Darwish, F Moukalled, L Mangani, and M Darwish. *The finite volume method*. Springer, 2016.
- [14] Kenneth H Huebner, Donald L Dewhurst, Douglas E Smith, and Ted G Byrom. *The finite element method for engineers*. John Wiley & Sons, 2001.
- [15] Uri M. Ascher, Steven J. Ruuth, and Raymond J. Spiteri. Implicit-explicit runge-kutta methods for time-dependent partial differential equations. *Applied Numerical Mathematics*, 25(2):151–167, 1997. Special Issue on Time Integration.
- [16] Karim M Abadir and Jan R Magnus. *Matrix algebra*, volume 1. Cambridge University Press, 2005.
- [17] Alexandros Nikolaos Ziogas, Tal Ben-Nun, Timo Schneider, and Torsten Koehnert. Npbench: A benchmarking suite for high-performance numpy. In *Proceedings of the ACM International Conference on Supercomputing*, pages 63–74, 2021.
- [18] Ilya Burylov, Michael Chuvelev, Bruce Greer, Greg Henry, Sergey Kuznetsov, and Boris Sabanin. Intel performance libraries: Multi-core-ready software for numeric-intensive computation. *Intel technology journal*, 11(4), 2007.
- [19] Parviz Moin and Krishnan Mahesh. Direct numerical simulation: a tool in turbulence research. *Annual review of fluid mechanics*, 30(1):539–578, 1998.

- [20] Jörg Schumacher. Sub-kolmogorov-scale fluctuations in fluid turbulence. *Europhysics Letters*, 80(5):54001, 2007.
- [21] James R Powell. The quantum limit to moore’s law. *Proceedings of the IEEE*, 96(8):1247–1248, 2008.
- [22] Karl Rupp and Siegfried Selberherr. The economic limit to moore’s law. *IEEE Transactions on Semiconductor Manufacturing*, 24(1):1–4, 2010.
- [23] Mark Horowitz and Emily Grumbling. Quantum computing: progress and prospects. 2019.
- [24] Frank Gaitan. Finding flows of a navier–stokes fluid through quantum computing. *npj Quantum Information*, 6(1):61, 2020.
- [25] Frank Gaitan. Finding solutions of the navier-stokes equations through quantum computing—recent progress, a generalization, and next steps forward. *Advanced Quantum Technologies*, 4(10):2100055, 2021.
- [26] Zhao-Yun Chen, Cheng Xue, Si-Ming Chen, Bing-Han Lu, Yu-Chun Wu, Ju-Chun Ding, Sheng-Hong Huang, and Guo-Ping Guo. Quantum approach to accelerate finite volume method on steady computational fluid dynamics problems. *Quantum Information Processing*, 21(4):137, 2022.
- [27] Szabolcs Jóczik, Zoltán Zimborás, Tamás Majoros, and Attila Kiss. A cost-efficient approach towards computational fluid dynamics simulations on quantum devices. *Applied Sciences*, 12(6):2873, 2022.
- [28] Wael Itani, Katepalli R Sreenivasan, and Sauro Succi. Quantum algorithm for lattice boltzmann (qalb) simulation of incompressible fluids with a nonlinear collision term. *Physics of Fluids*, 36(1), 2024.
- [29] Sauro Succi, Wael Itani, Claudio Sanavio, Katepalli R Sreenivasan, and René Steijl. Ensemble fluid simulations on quantum computers. *Computers & Fluids*, 270:106148, 2024.
- [30] Xiangyu Li, Xiaolong Yin, Nathan Wiebe, Jaehun Chun, Gregory K Schenter, Margaret S Cheung, and Johannes Müllenstädt. Potential quantum advantage for simulation of fluid dynamics. *arXiv preprint arXiv:2303.16550*, 2023.
- [31] Frank Arute, Kunal Arya, Ryan Babbush, Dave Bacon, Joseph C Bardin, Rami Barends, Rupak Biswas, Sergio Boixo, Fernando GSL Brandao, David A Buell, et al. Quantum supremacy using a programmable superconducting processor. *Nature*, 574(7779):505–510, 2019.
- [32] Suguru Endo, Zhenyu Cai, Simon C Benjamin, and Xiao Yuan. Hybrid quantum-classical algorithms and quantum error mitigation. *Journal of the Physical Society of Japan*, 90(3):032001, 2021.
- [33] Iulia Buluta and Franco Nori. Quantum simulators. *Science*, 326(5949):108–111, 2009.
- [34] Ehud Altman, Kenneth R Brown, Giuseppe Carleo, Lincoln D Carr, Eugene Demler, Cheng Chin, Brian DeMarco, Sophia E Economou, Mark A Eriksson, Kai-Mei C Fu, et al. Quantum simulators: Architectures and opportunities. *PRX quantum*, 2(1):017003, 2021.
- [35] Luigia Carlucci Aiello. The multifaceted impact of ada lovelace in the digital age. *Artificial Intelligence*, 235:58–62, 2016.
- [36] Christopher Hollings, Ursula Martin, and Adrian Clifford Rice. *Ada Lovelace: The making of a computer scientist*, volume 85024040. Bodleian Library Oxford, 2018.
- [37] Bojia Duan, Jiabin Yuan, Chao-Hua Yu, Jianbang Huang, and Chang-Yu Hsieh. A survey on hhl algorithm: From theory to application in quantum machine learning. *Physics Letters A*, 384(24):126595, 2020.
- [38] Andrés Gilyén, Yuan Su, Guang Hao Low, and Nathan Wiebe. Quantum singular value transformation and beyond: exponential improvements for quantum matrix arithmetics. In *Proceedings of the 51st Annual ACM SIGACT Symposium on Theory of Computing*, pages 193–204, 2019.
- [39] Andrew M Childs, Robin Kothari, and Rolando D Somma. Quantum algorithm for systems of linear equations with exponentially improved dependence on precision. *SIAM Journal on Computing*, 46(6):1920–1950, 2017.
- [40] Leigh Lapworth. A hybrid quantum-classical cfd methodology with benchmark hhl solutions. *arXiv preprint arXiv:2206.00419*, 2022.
- [41] Romina Yalovetzky, Pierre Minssen, Dylan Herman, and Marco Pistoia. Hybrid hhl with dynamic quantum circuits on real hardware. *arXiv preprint arXiv:2110.15958*, 2021.
- [42] Carlos Bravo-Prieto, Ryan LaRose, Marco Cerezo, Yigit Subasi, Lukasz Cincio, and Patrick J Coles. Variational quantum linear solver. *Quantum*, 7:1188, 2023.
- [43] YY Liu, Zhen Chen, Chang Shu, Siou Chye Chew, Boo Cheong Khoo, Xiang Zhao, and YD Cui. Application of a variational hybrid quantum-classical algorithm to heat conduction equation and analysis of time complexity. *Physics of Fluids*, 34(11), 2022.
- [44] Hai-Ling Liu, Yu-Sen Wu, Lin-Chun Wan, Shi-Jie Pan, Su-Juan Qin, Fei Gao, and Qiao-Yan Wen. Variational quantum algorithm for the poisson equation. *Physical Review A*, 104(2):022418, 2021.
- [45] Mazen Ali and Matthias Kabel. Performance study of variational quantum algorithms for solving the poisson equation on a quantum computer. *Physical Review Applied*, 20(1):014054, 2023.
- [46] René Steijl and George N Barakos. Parallel evaluation of quantum algorithms for computational fluid dynamics. *Computers & Fluids*, 173:22–28, 2018.
- [47] René Steijl. Quantum algorithms for fluid simulations. *Advances in quantum communication and information*, 31, 2019.
- [48] VK Srivastava and M Tamsir. Crank-nicolson semi implicit approach for numerical solutions of two-dimensional coupled nonlinear burgers’ equations. *International Journal of Applied Mechanics and Engineering*, 17(2):571, 2012.
- [49] Vijitha Mukundan and Ashish Awasthi. Linearized implicit numerical method for burgers’ equation. *Nonlinear Engineering*, 5(4):219–234, 2016.
- [50] Vijitha Mukundan and Ashish Awasthi. Efficient numerical techniques for burgers’ equation. *Applied Mathematics and Computation*, 262:282–297, 2015.
- [51] Cuilian You, Yan Cheng, and Hongyan Ma. Stability of euler methods for fuzzy differential equation. *Symmetry*, 14(6):1279, 2022.
- [52] Thomas Y Hou and Zuoqiang Shi. An efficient semi-implicit immersed boundary method for the navier–stokes equations. *Journal of Computational Physics*, 227(20):8968–8991, 2008.
- [53] Qinqing Zou. Gmres algorithms over 35 years. *Applied Mathematics and Computation*, 445:127869, 2023.
- [54] R.A. Horn and C.R. Johnson. *Matrix Analysis*. Matrix Analysis. Cambridge University Press, 2013.
- [55] A Refik Bahadır. A fully implicit finite-difference scheme for two-dimensional burgers’ equations. *Applied Mathematics and Computation*, 137(1):131–137, 2003.
- [56] Yuhang Fu, Weiqi Shen, Jiahuan Cui, Yao Zheng, Guangwen Yang, Zhao Liu, Jifa Zhang, Tingwei Ji, Fangfang Xie, Xiaojing Lv, et al. Towards exascale computation for turbomachinery flows. *arXiv preprint arXiv:2308.06605*, 2023.